iScience, Volume *24*

Supplemental information

$CD27^{hi}CD38^{hi}$ plasmablasts are activated B cells of mixed origin with distinct function

Angeline Rouers, Ramapraba Appanna, Marion Chevrier, Josephine Lum, Mai Chan Lau, Lingqiao Tan, Thomas Loy, Alicia Tay, Raman Sethi, Durgalakshmi Sathiakumar, Kaval Kaur, Julia Böhme, Yee-Sin Leo, Laurent Renia, Shanshan W. Howland, Amit Singhal, Jinmiao Chen, and Katja Fink

Supplementary Figure S1

A

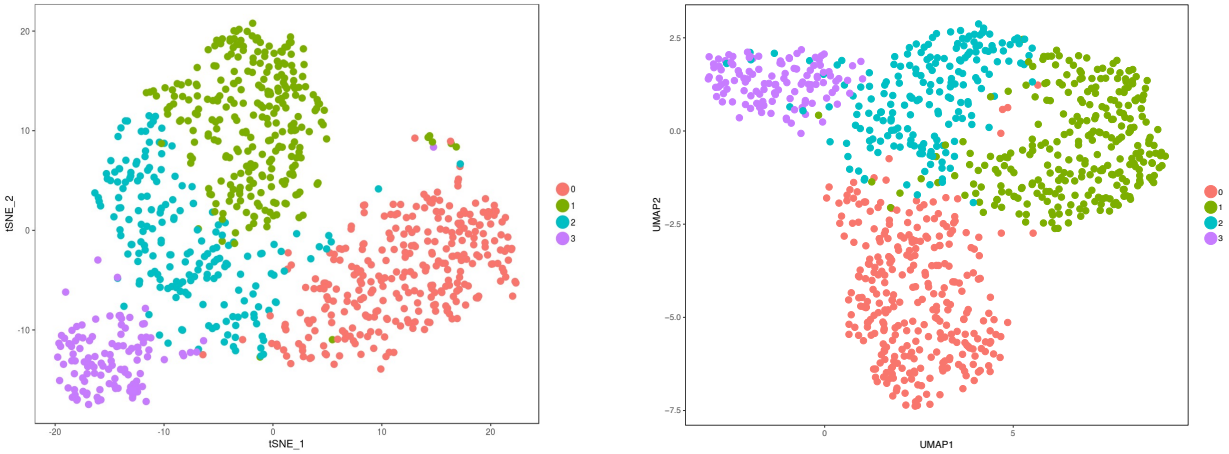

B

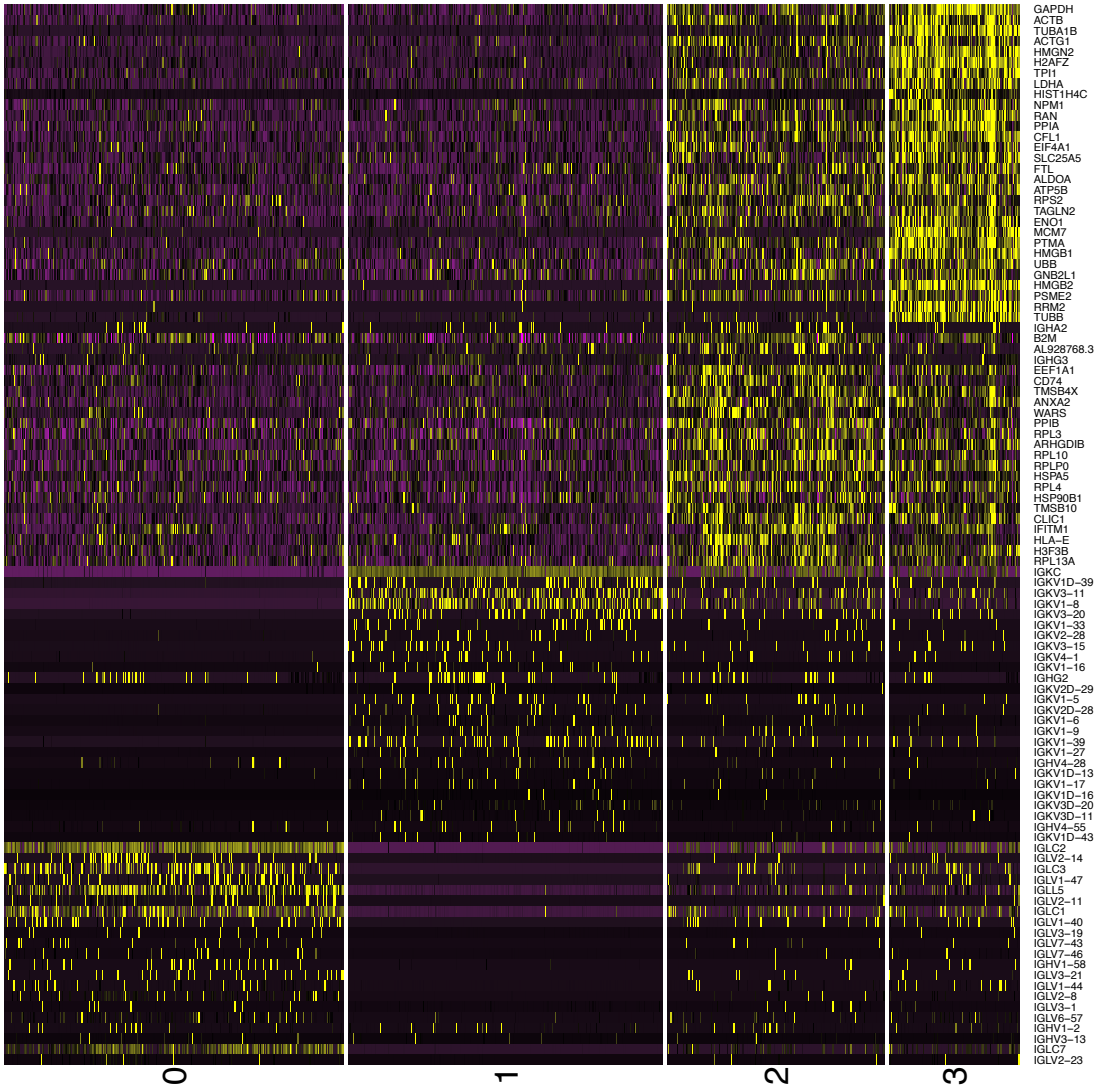

Supplementary Figure S1: Clusters obtained using different algorithms and differences between clusters 0 and 1. A) Transcriptome from 890 single plasmablasts from 5 patients (1 primary and 4 secondary infections) were used for the analysis. tSNE plot (left) and UMAP plot (right) using the 400 most variable genes from Singular. B) Heatmap showing the DEGs between cluster 0 and 1. Related to Figure 1.

Supplementary Figure S2

A

Patient ID	Cluster 0/1	Cluster 2	Cluster 3	Total
E1481DK2 (NA)	7	3	6	16
LNA002 (V1)	-	-	-	-
LNA002 (V2)	100	59	22	181
LNA006 (V1)	85	24	39	148
LNA006 (V2)	142	30	16	188
LNA018 (V1)	24	37	12	73
LNA018 (V2)	155	24	9	188
LNA036 (V1)	-	-	-	-
LNA036 (V2)	68	16	12	96

B

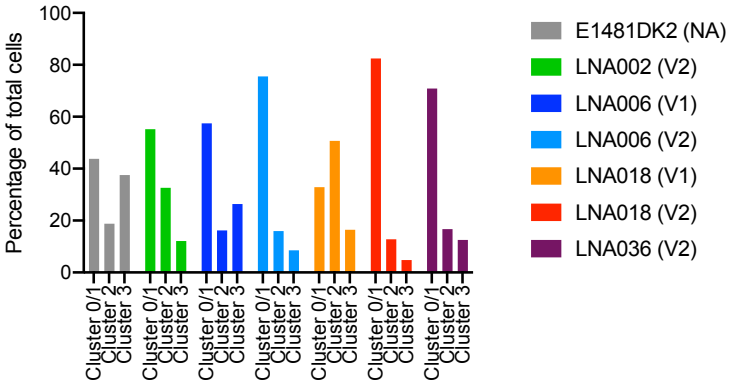

C

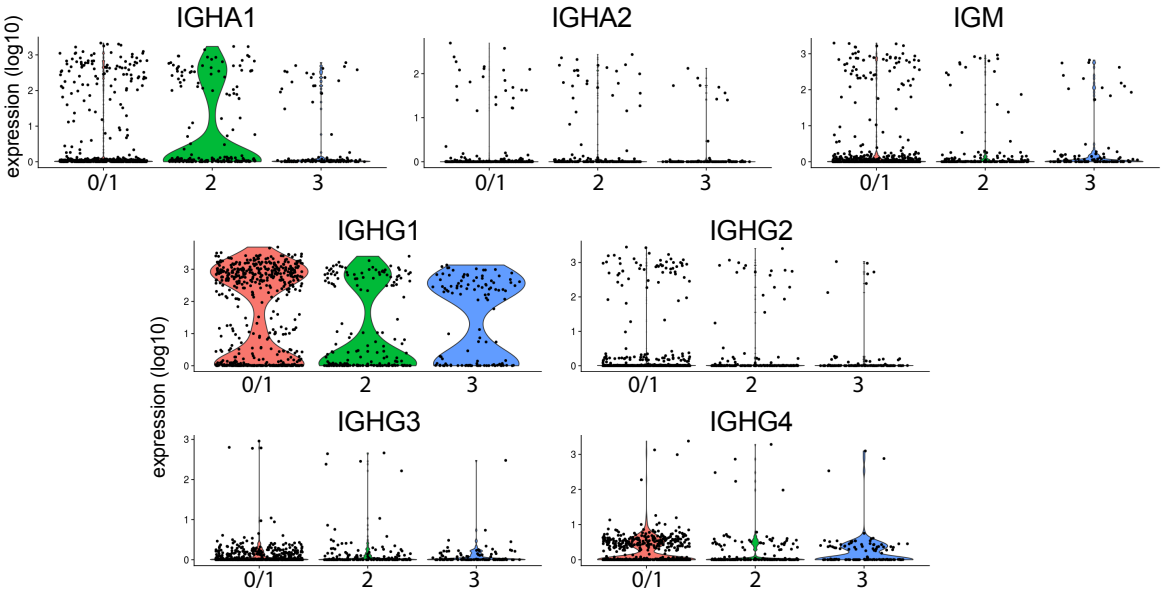

Supplementary Figure S2: Cluster distribution and heavy chain isotype usage in plasmablast clusters. A) Number of cells with scRNAseq data per patient sample and timepoint. The visit number is indicated in brackets for each sample. NA: not applicable. B) Normalized cluster size per patient sample and timt point. C) Violin plots of the expression of each antibody isotype IGHA1 (IgA1), IGHA2 (IgA2), IGM (IgM), IGHG1 (IgG1), IGHG2 (IgG2), IGHG3 (IgG3) and IGHG4 (IgG4) is represented for individual plasmablasts (n=890) according to their cluster (0/1:red, 2: green, 3:blue). Related to Figure 1.

Supplementary Figure S3

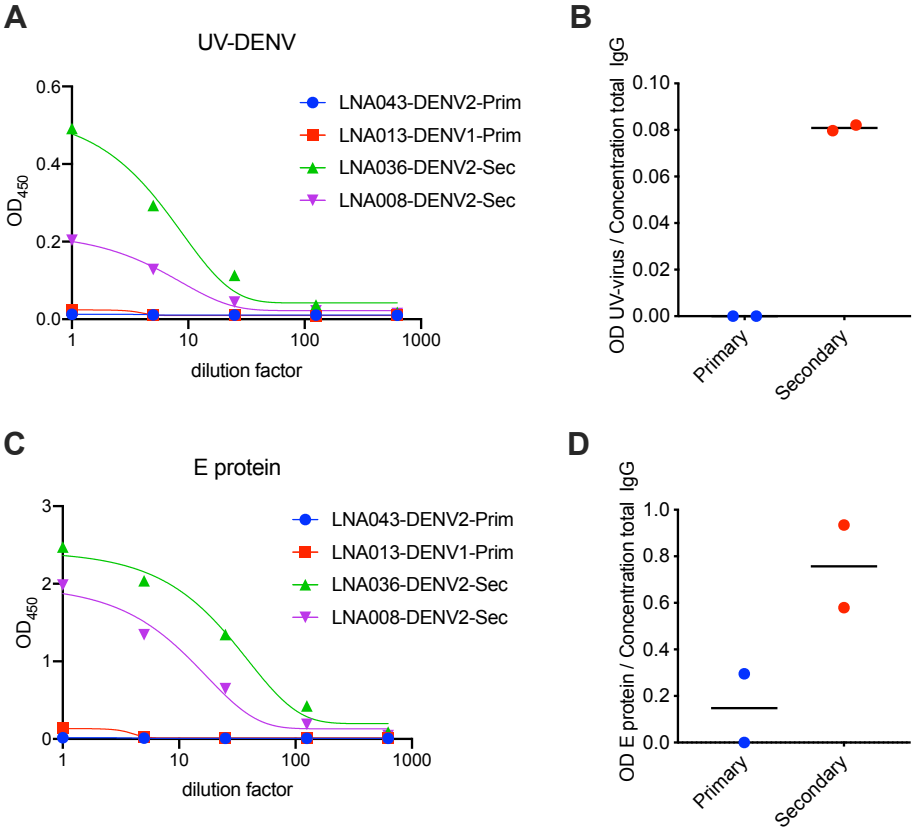

Supplementary Figure S3: Specificity of antibodies secreted from bulk-sorted plasmablasts from primary and secondary patients. A-D) Plasmablasts ($CD19^{+}IgD^{-}CD38^{+}CD27^{+}$) from two primary and two secondary patients early after dengue-infection (6-10 days post-fever) were sorted and cultured for 24h before collection of cell culture supernatant containing secreted antibodies. ELISA was performed to detect DENV-specific IgG binding to UV-inactivated DENV (A and B) or E protein (C and D) of the serotype of the current infection. B and D: OD-values for specific binding at 5x dilution (linear range of the dilution curve) were normalized to the concentration of total IgG detected in the supernatants. Each symbol represents one patient, the mean is indicated with a bar in (B) and (D). Samples were tested in duplicates . Related to Figure 2.

Supplementary Figure S4

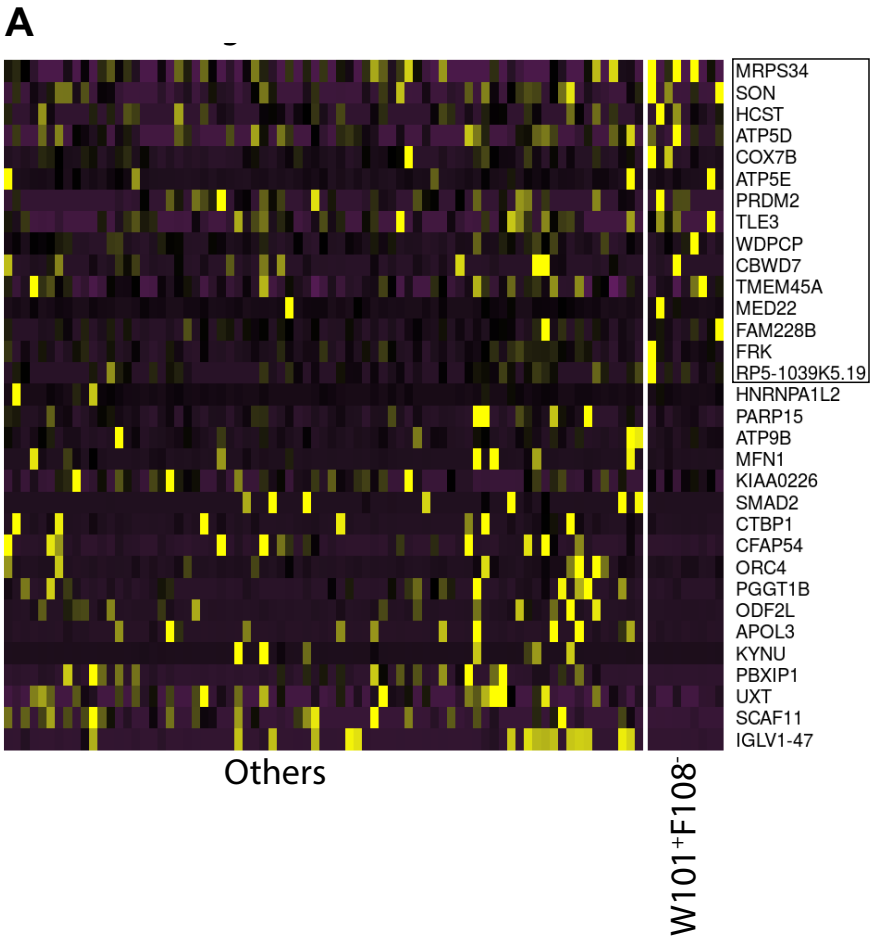

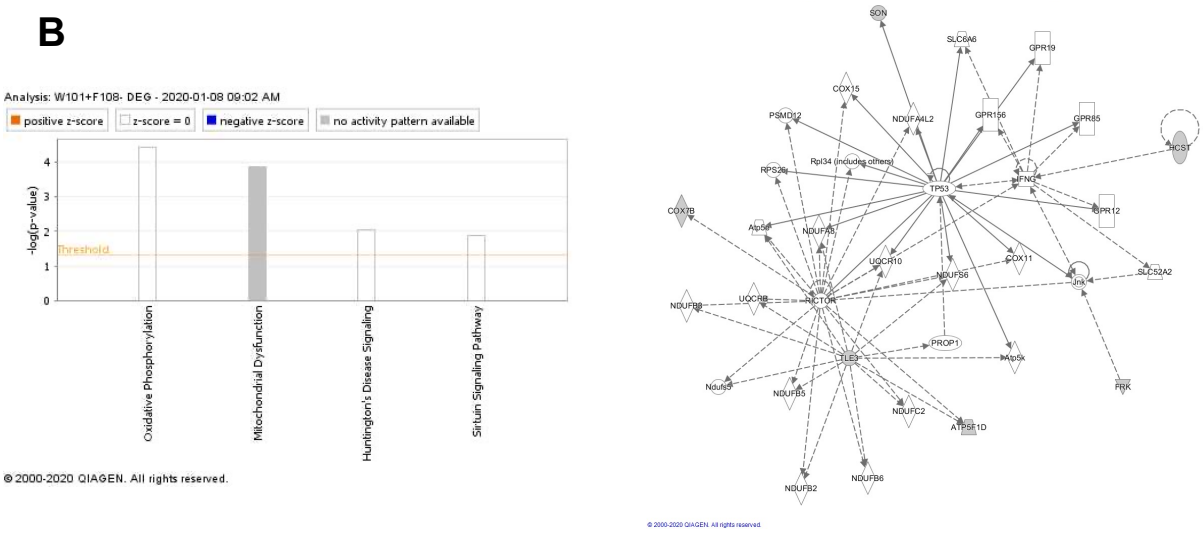

Supplementary Figure S4: Fusion loop W101⁺F108⁻ plasmablast-derivate mAbs show a higher metabolic gene expression profile. A) Gene expression in W101⁺F108⁻ mAbs compared to others. **B)** Most significant pathways (left) for the 15 genes framed in panel A and the network (right) including the highest number of theses genes (n=6, genes of interest are indicated in grey). Ingenuity software (Qiagen) was used. For the network: dotted lines represent indirect interactions and solid lines represent direct interaction. Directions of the arrows represent the sense of the interaction. Related to Figure 2.

Supplementary Figure S5

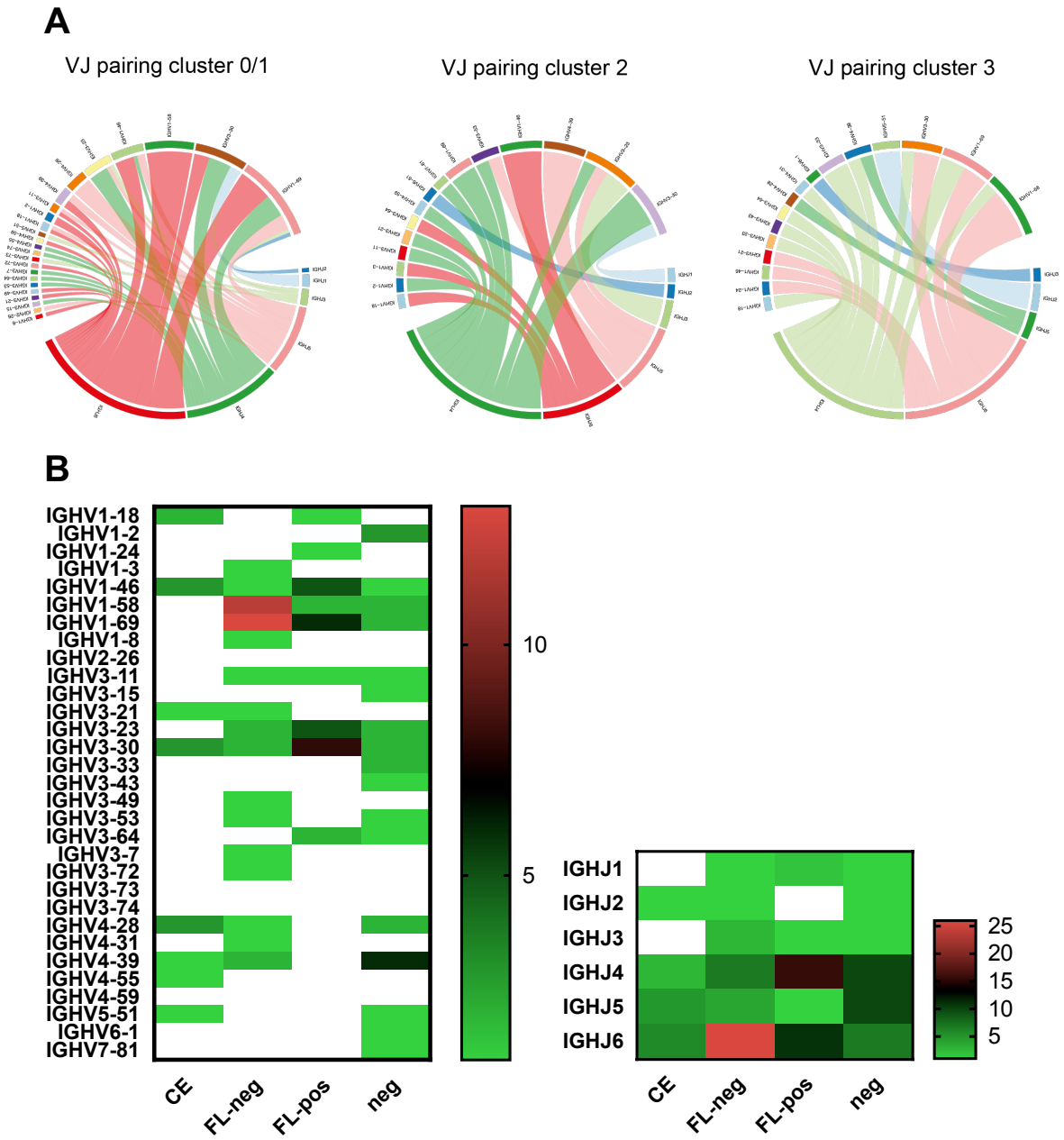

Supplementary Figure S5: VDJ usage of mAbs expressed from clusters 0/1, 2 and 3. A) Linkage of V gene and J gene usage for each cluster. Plots were generated with VDJtools (PlotFancyVJUsage) (https://vdjtools-doc.readthedocs.io). B) Individual V gene usage and J gene usage for antibodies per binding class: CE: complex epitope, FL-neg: fusionloop negative, FL-pos: fusionloop positive, neg: non-dengue. The color code for the heatmaps in indicated, units are number of antibodies. Related to Figure 2.

Supplementary Figure S6

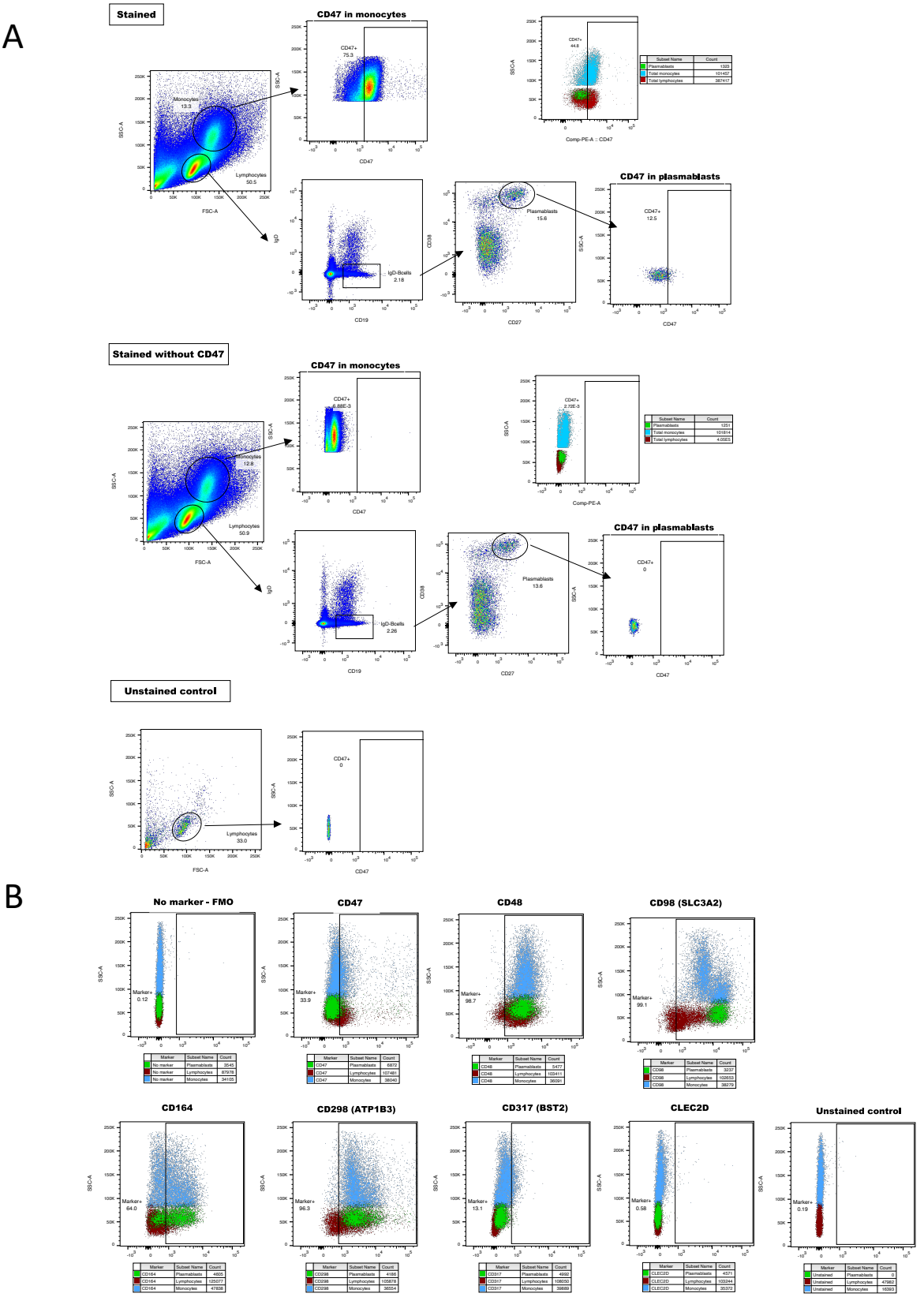

Supplementary Figure S6: Surface expression of markers differentially expressed in cluster 2 and 3 compared to cluster 0/1. A) Plasmablast surface protein expression of seven markers that were differentially expressed in clusters 2 and 3 versus clusters 0/1. An overlay of surface marker expression on lymphocytes, monocytes and plasmablasts is shown for reference. **B**) Gating for CD47^{+} plasmablasts for a fully stained sample, stain without CD47 (fluorescence minus one FMO) and unstained control. CD47 expression on monocytes was used as a reference to set the CD47 gate. An overlay of CD47 expression on lymphocytes, monocytes and plasmablasts is shown for reference. Related to Figure 3.

Supplementary Figure S7

A

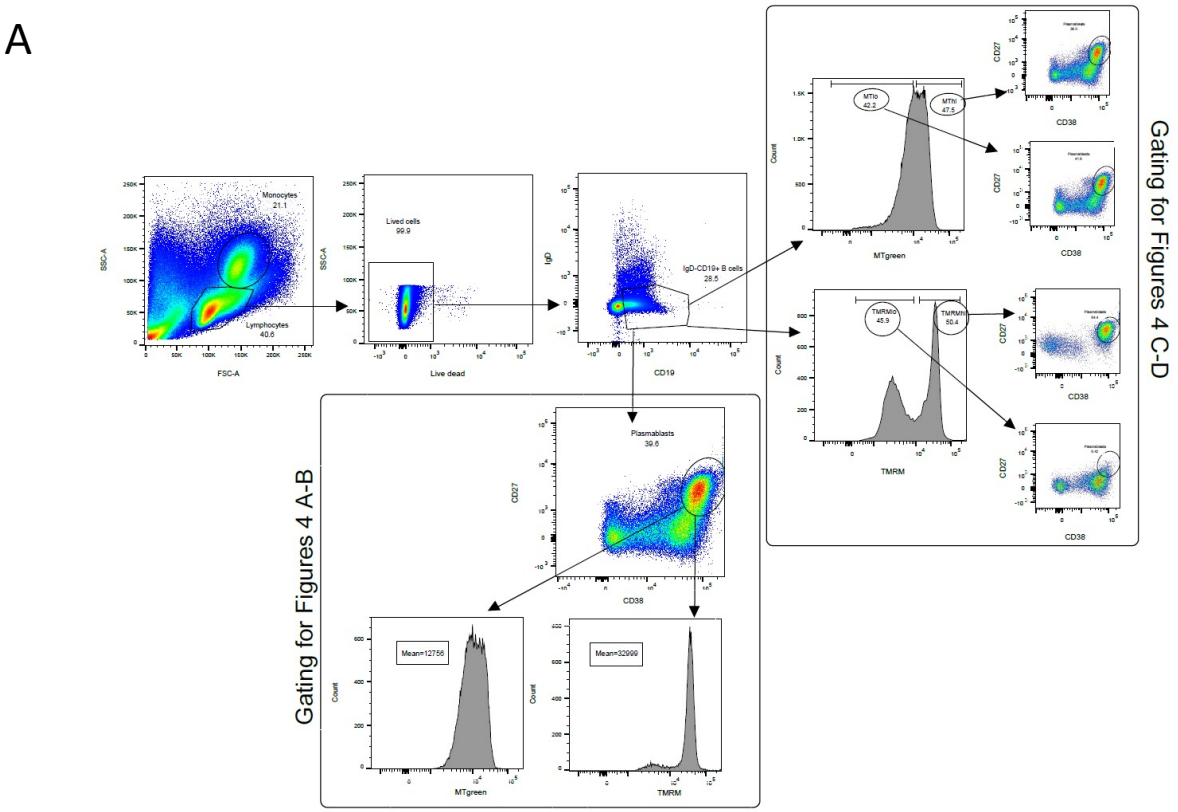

B

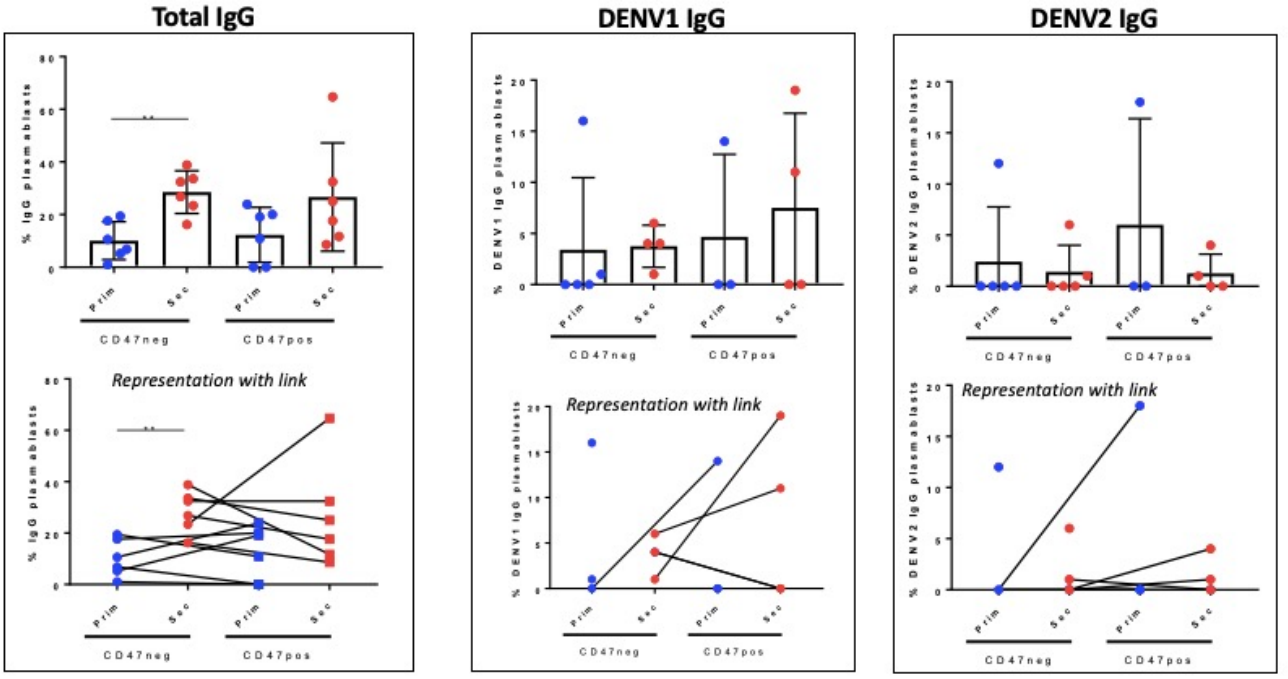

Supplementary Figure S7: Gating strategy for MT and TMRM content and antibody secretion of CD47⁺ and CD47⁻ plasmablasts detected by ELISPOT. A) Gating strategy for the identification of MT or TMRM high and –low plasmabasts. This gating was used for the data illustrated in Figure 4A-B and 4D-E. B) Total IgG-secreting cells, and DENV-1 E protein or DENV-2 E protein specific IgG secreting cells, calculated as a percentage of input sorted plasmablasts. Each symbol represents one donor; the lower panel of graphs links CD47⁺ and CD47⁻ plasmablasts from the same donor. Bars represent means±SD, ** p=0.0019. Students t test. Data are combined from three independent experiments. Related to Figure 4.

Supplementary Figure S8

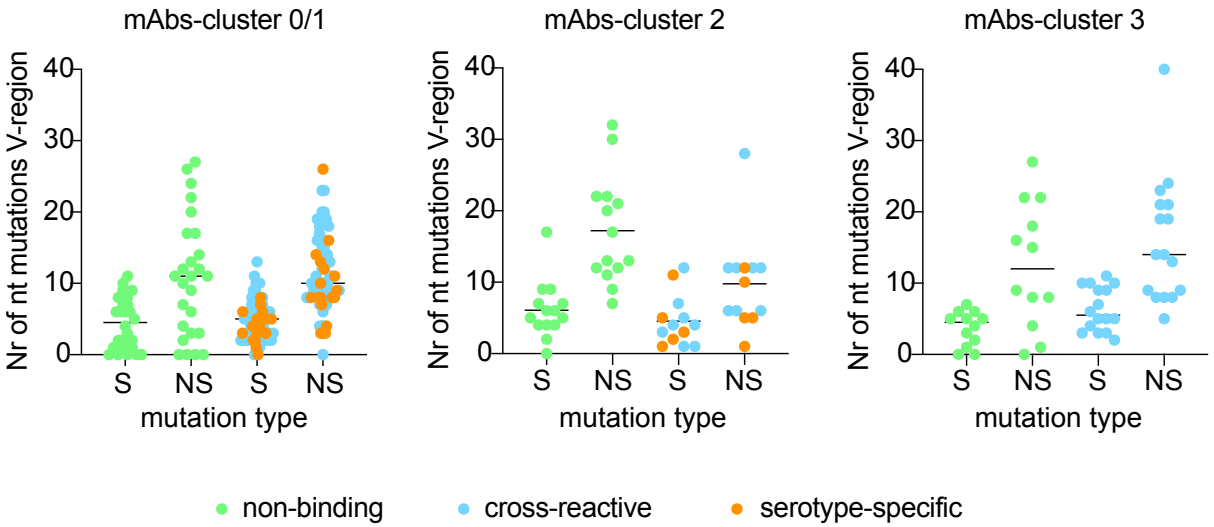

Supplementary Figure S8: Mutation analysis of antibodies from clusters 0/1, 2 and 3. The number of nucleotide mutations in the V region as determined by highV-Quest, IMGT, using sequences assembled from RNAseq data using basic algorithm. S: silent, NS: non-silent. Each symbol represents one antibody sequence. The mean is indicated with a bar. Related to Figure 6.

Supplementary Figure S9

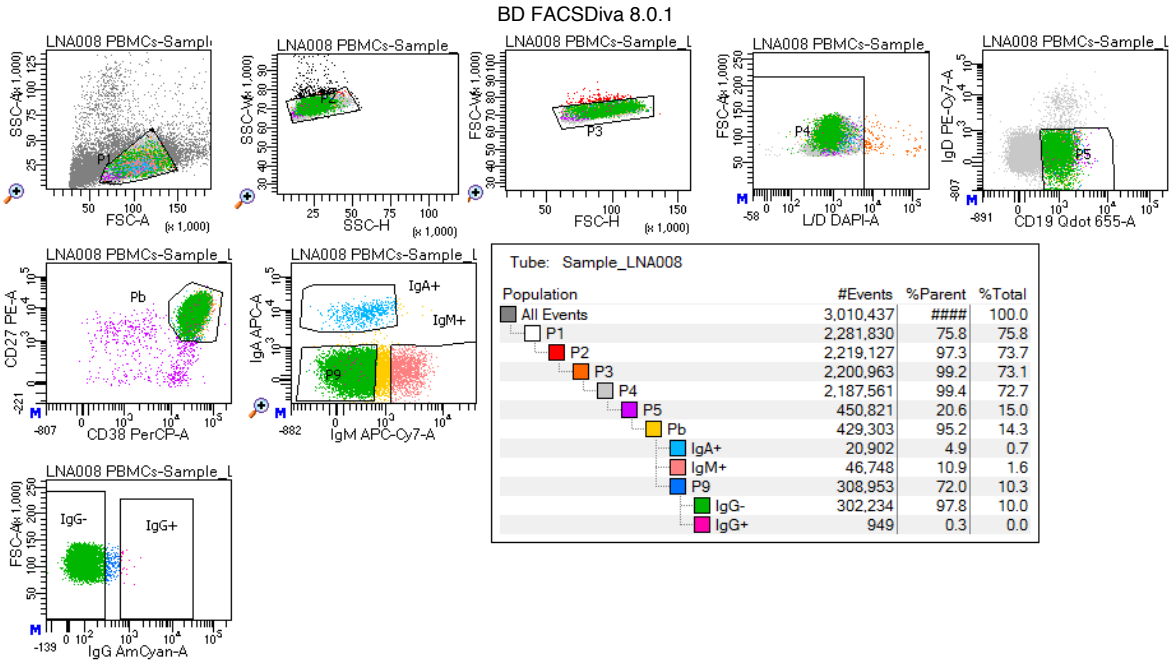

Supplementary Figure S9: Gating strategy for the sorting of plasmablasts based on Ig surface expression. IgA+, IgM+, IgG+ and IgG- populations were sorted for the analysis shown in Figure 7. Related to Figure 7.

Supplementary Table S1: 100 top DEG between cluster 3 and clusters 0/1 and 2. Related to Figure 1.

	p_val	avg_logFC	pct.1	pct.2	p_val_adj	cluster	gene
MT-CYB.2	4.46E-09	0.23914208	1	0.997	8.82E-05	3	MT-CYB
GAPDH.2	1.38E-90	0.20292327	1	0.974	2.73E-86	3	GAPDH
ACTB.2	3.60E-61	0.19496342	1	0.984	7.13E-57	3	ACTB
MT-ND4L.2	6.33E-11	0.18859622	1	1	1.25E-06	3	MT-ND4L
MT-CO1.2	4.62E-07	0.15491057	1	1	0.00914092	3	MT-CO1
TUBA1B.2	1.42E-165	0.13086787	0.983	0.359	2.82E-161	3	TUBA1B
MT-RNR2.2	5.53E-07	0.12370244	1	1	0.01094717	3	MT-RNR2
MT-ND4.2	3.74E-12	0.11013875	1	1	7.40E-08	3	MT-ND4
ACTG1.2	1.07E-38	0.10025465	0.983	0.907	2.11E-34	3	ACTG1
MT-RNR1.1	4.99E-12	0.09711459	1	0.999	9.88E-08	3	MT-RNR1
HMGN2.2	2.77E-111	0.0967229	1	0.766	5.49E-107	3	HMGN2
MT-ATP6.2	6.86E-07	0.09367726	1	0.997	0.01357116	3	MT-ATP6
MT-CO3.2	8.32E-07	0.07736197	1	0.994	0.01646792	3	MT-CO3
H2AFZ.2	3.65E-160	0.07500873	0.974	0.702	7.22E-156	3	H2AFZ
MT-ATP8.2	1.29E-06	0.06642868	0.966	0.889	0.02558412	3	MT-ATP8
TMSB4X.2	6.24E-18	0.05974827	1	0.977	1.24E-13	3	TMSB4X
TPI1.2	9.38E-69	0.0566308	0.974	0.745	1.86E-64	3	TPI1
LDHA.2	2.02E-73	0.05621023	0.974	0.712	4.00E-69	3	LDHA
HIST1H4C.2	0	0.05490892	0.957	0.488	0	3	HIST1H4C
NPM1.2	1.78E-52	0.05438048	0.974	0.922	3.52E-48	3	NPM1
RAN.2	1.23E-73	0.05372681	0.983	0.691	2.44E-69	3	RAN
PPIA.2	1.51E-54	0.05370807	0.991	0.948	2.98E-50	3	PPIA
CFL1.2	1.24E-59	0.05249302	0.991	0.934	2.46E-55	3	CFL1
EIF4A1.2	6.19E-41	0.0521868	0.983	0.868	1.23E-36	3	EIF4A1
SLC25A5.2	1.01E-62	0.05071855	0.974	0.769	2.00E-58	3	SLC25A5
FTL.2	1.51E-29	0.0498335	0.983	0.994	2.98E-25	3	FTL
ALDOA.2	1.84E-48	0.04970299	0.983	0.82	3.65E-44	3	ALDOA
ARHGDIB.2	1.15E-17	0.04524813	1	0.941	2.28E-13	3	ARHGDIB
ANXA2.2	9.01E-12	0.04512537	0.991	0.924	1.78E-07	3	ANXA2
ATP5B.2	7.55E-26	0.04459195	0.974	0.913	1.49E-21	3	ATP5B
MT-ND5.2	6.82E-20	0.04432886	1	0.992	1.35E-15	3	MT-ND5
RPS2.2	3.88E-18	0.04286263	1	0.955	7.68E-14	3	RPS2
TAGLN2.2	1.34E-26	0.04220326	0.974	0.862	2.65E-22	3	TAGLN2
RPLP0.2	3.50E-17	0.04166771	1	0.987	6.93E-13	3	RPLP0
ENO1.2	7.33E-76	0.04120131	0.974	0.765	1.45E-71	3	ENO1
MCM7.2	5.21E-82	0.040564	0.94	0.233	1.03E-77	3	MCM7
PTMA.2	6.84E-88	0.04034366	1	0.979	1.35E-83	3	PTMA
HMGB1.2	5.17E-79	0.03977241	1	0.947	1.02E-74	3	HMGB1
UBB.2	1.00E-21	0.03976571	1	0.982	1.98E-17	3	UBB
GNB2L1.2	6.69E-13	0.0394505	1	0.957	1.32E-08	3	GNB2L1
HMGB2.2	6.14E-97	0.03837239	0.966	0.155	1.22E-92	3	HMGB2
PSME2.2	1.20E-26	0.03736866	0.991	0.926	2.37E-22	3	PSME2
RRM2.2	1.02E-88	0.03672434	0.853	0.071	2.02E-84	3	RRM2
TMSB10.2	4.77E-27	0.0365712	1	0.984	9.43E-23	3	TMSB10
TUBB.2	6.65E-115	0.03608732	0.931	0.278	1.32E-110	3	TUBB
RPL4.2	3.92E-14	0.03441241	0.991	0.961	7.75E-10	3	RPL4
RPS3.2	6.30E-14	0.03359699	1	0.983	1.25E-09	3	RPS3
RPSA.2	1.02E-25	0.03358494	0.983	0.833	2.03E-21	3	RPSA
CORO1A.2	2.34E-32	0.03278004	0.966	0.677	4.63E-28	3	CORO1A

EEF1G.2	1.73E-16	0.03246396	0.991	0.982	3.42E-12	3	EEF1G
HNRNPA1.2	8.63E-17	0.0314516	0.983	0.937	1.71E-12	3	HNRNPA1
RPL7.2	5.09E-17	0.0313974	1	0.973	1.01E-12	3	RPL7
RPL41.2	7.71E-28	0.03133105	1	0.997	1.52E-23	3	RPL41
EBP.1	8.44E-34	0.0311768	0.81	0.389	1.67E-29	3	EBP
PSMB4.2	2.02E-15	0.03071009	0.991	0.841	4.00E-11	3	PSMB4
PFN1.2	1.24E-91	0.03001196	0.991	0.97	2.46E-87	3	PFN1
ATP5A1.2	1.31E-18	0.02999555	1	0.968	2.59E-14	3	ATP5A1
LDHB.2	1.20E-35	0.02982546	0.94	0.758	2.37E-31	3	LDHB
LSP1.2	2.42E-13	0.02840182	1	0.93	4.79E-09	3	LSP1
CLIC1.2	1.90E-13	0.02796548	0.991	0.919	3.77E-09	3	CLIC1
HSPA8.2	3.04E-10	0.02785909	0.983	0.925	6.01E-06	3	HSPA8
RPL8.2	6.39E-12	0.02784662	1	0.99	1.26E-07	3	RPL8
OAZ1.2	4.19E-21	0.02780908	0.991	0.99	8.28E-17	3	OAZ1
RPL5.2	9.26E-14	0.02768101	0.991	0.953	1.83E-09	3	RPL5
PCNA.2	2.33E-83	0.0274815	0.802	0.076	4.61E-79	3	PCNA
PGAM1.2	8.21E-49	0.02729135	0.931	0.603	1.63E-44	3	PGAM1
FTH1.2	1.23E-16	0.02678318	1	0.97	2.43E-12	3	FTH1
SUB1.2	3.81E-11	0.02661373	1	0.997	7.55E-07	3	SUB1
HNRNPA2B1.2	2.87E-57	0.02607023	0.991	0.82	5.67E-53	3	HNRNPA2B1
CALM2.2	7.09E-24	0.02594923	0.931	0.767	1.40E-19	3	CALM2
CALM1.2	4.06E-23	0.02594184	0.991	0.938	8.03E-19	3	CALM1
H3F3B.2	2.63E-08	0.0256402	0.983	0.965	0.00051946	3	H3F3B
EIF4A3.1	1.22E-55	0.02532284	0.871	0.274	2.41E-51	3	EIF4A3
STMN1.2	8.06E-87	0.02502553	0.897	0.163	1.59E-82	3	STMN1
RPS5.2	1.37E-13	0.02464906	0.974	0.95	2.72E-09	3	RPS5
RPS3A.2	1.82E-10	0.02453792	1	0.994	3.61E-06	3	RPS3A
RPS18.2	1.10E-18	0.02437291	1	0.996	2.18E-14	3	RPS18
CYC1.2	2.56E-34	0.02432702	0.931	0.612	5.06E-30	3	CYC1
SLC25A3.2	4.47E-10	0.02335933	0.94	0.779	8.84E-06	3	SLC25A3
SMC4.2	1.07E-52	0.02324347	0.94	0.363	2.12E-48	3	SMC4
PDIA6.2	5.30E-10	0.02314873	0.991	0.974	1.05E-05	3	PDIA6
ARPC2.2	2.73E-13	0.02313993	0.983	0.966	5.40E-09	3	ARPC2
CHCHD2.2	2.02E-32	0.02295726	0.991	0.897	4.00E-28	3	CHCHD2
UQCRC1.2	1.61E-16	0.0228305	0.836	0.619	3.19E-12	3	UQCRC1
DDX39A.2	4.77E-38	0.02270163	0.879	0.411	9.43E-34	3	DDX39A
HNRNPC.2	1.35E-17	0.02261847	0.983	0.833	2.67E-13	3	HNRNPC
ANP32E.2	2.99E-81	0.02250432	0.94	0.654	5.91E-77	3	ANP32E
PSMA4.2	5.05E-24	0.02228402	0.931	0.685	9.99E-20	3	PSMA4
RPS6.2	1.77E-14	0.02177789	1	0.987	3.50E-10	3	RPS6
SELT.2	4.22E-11	0.02160166	0.94	0.798	8.35E-07	3	SELT
PSMB8.2	9.47E-09	0.02101971	0.905	0.798	0.00018728	3	PSMB8
MYL6.2	1.12E-10	0.02090649	1	0.984	2.21E-06	3	MYL6
PGK1.2	5.42E-16	0.0206908	0.966	0.782	1.07E-11	3	PGK1
MT-ND6.2	2.72E-17	0.02019391	0.983	0.915	5.39E-13	3	MT-ND6
EIF1.2	1.93E-08	0.02006964	0.983	0.959	0.00038089	3	EIF1
RPL19.2	4.03E-13	0.02006737	1	0.977	7.98E-09	3	RPL19
EWSR1.2	4.06E-10	0.01992959	0.948	0.827	8.02E-06	3	EWSR1
ATP5F1.2	5.79E-08	0.01967873	0.828	0.63	0.00114544	3	ATP5F1
RPL7A.2	1.59E-12	0.01912488	1	0.926	3.14E-08	3	RPL7A
SRSF3.2	1.69E-28	0.01911537	0.983	0.867	3.35E-24	3	SRSF3